



Heterogeneous Fenton process using iron-containing waste (ICW) for methyl orange degradation: process performance and modeling

Mohamed E.M. Ali^a, Tarek A. Gad-Allah^a, Emad S. Elmolla^{b,*}, Mohamed I. Badawy^a

^aWater Pollution Research Department, National Research Centre, Cairo, Egypt

^bDepartment of Civil Engineering, Faculty of Engineering, Al-Azhar University, Cairo, Egypt

Tel. +20 1113301981; emails: em_civil@yahoo.com; emadelmolla@yahoo.com

Received 7 June 2012; Accepted 2 May 2013

ABSTRACT

The feasibility of using iron-containing waste (ICW) as new low-cost heterogeneous Fenton catalyst for methyl orange (MO) degradation has been studied. Process modeling and simulation has been conducted using artificial neural network (ANN). Complete degradation of MO was achieved at 0.2 g/L ICW concentration, 24 mM H₂O₂ dose, and pH 2 in 30 min. A three-layered back-propagation neural network with tangent sigmoid transfer function (*tansig*) at hidden layer and linear transfer function (*purelin*) at output layer was used for modeling the process performance. ANN-predicted results are very close to the experimental results with a correlation coefficient (R^2) of 0.961 and a mean squared error of 0.039. The sensitivity analysis showed that all studied variables (reaction time, ICW concentration, H₂O₂ dose, pH, and MO concentration) have strong effect on MO degradation. Among all studied variables, pH appeared to be the most influential input variable followed by ICW concentration.

Keywords: Artificial neural network (ANN); Modeling; Iron-containing waste; Heterogeneous Fenton; Degradation; Methyl orange

1. Introduction

Effluents from textile industrial activities usually contain several classes of hazardous dyes that have negative effect on water resources, human health, and environment. These effluents not only deteriorate the receiving water, but also pose significant threats to aquatic life because of oxygen deficiency and formation of some toxic products. Most of textile dyes are designed to produce long-lasting colors and are resistant to mild oxidation conditions. Therefore, stronger oxidation agents such as Fenton's reagent could be

used for the degradation of dye structure [1]. It was estimated that over 700,000 tons of dyes and pigments are produced annually and about 20% of dyes find their way to the environment due to inefficient use [2].

Development of an efficient process for dyes degradation is needed to overcome problems associated with traditional processes. Advanced oxidation processes (AOPs) rely on the generation of extremely active hydroxyl ($\cdot\text{OH}$) radicals, which are identified as strong and nonselective oxidants for degradation of almost all organic compounds [3]. One of the AOPs is Fenton-like (heterogeneous Fenton) process which

*Corresponding author.

generates powerful $\cdot\text{OH}$ radicals from H_2O_2 in the presence of iron ($\text{Fe}^{2+}/\text{Fe}^{3+}/\text{H}_2\text{O}_2$) [1]. In the heterogeneous Fenton reaction, soluble Fe^{2+} (catalyst) may be replaced by iron-containing waste (ICW) produced from steel industries.

Steel is manufactured by the chemical reduction of iron or using an integrated steel manufacturing process or a direct reduction process. In the conventional integrated steel manufacturing process, the iron from the blast furnace is converted to steel in a basic oxygen furnace. Steel can also be made in an electric arc furnace from scrap steel and, in some cases, from direct reduced iron. Three major waste streams are generated during steel manufacturing: air emission, wastewater, and solid waste. The amount of the generated solid waste from the conventional process (furnace slag, collected dust) is in the range of 300–500 kg/t of steel manufactured. This ICW is rich in iron and can be used as a catalyst in heterogeneous Fenton process for wastewater treatment.

The use of ICW as heterogeneous Fenton catalyst may give numerous advantages over the classic heterogeneous/homogeneous Fenton catalysts. In case of comparison with homogeneous Fenton catalysts, these advantages are less sludge production and easy separation of the catalyst [4,5]. However, it is a cost-effective catalyst when compared with other heterogeneous Fenton catalysts such as Fe_2O_3 , S-doped Fe_2O_3 , Fe_3O_4 [6–11].

The objective of this work is to examine the feasibility of using ICW as a new low-cost heterogeneous Fenton catalyst for methyl orange (MO) degradation. Process modeling and simulation using artificial neural network (ANN) are investigated. The ANN modeling outputs are compared with the experimental data.

2. Experimental

2.1. Reagents

All chemicals used in this study were of analytical grade and were used without further purification. The ICW was collected from the Egyptian for iron and steel Company and was used after grinding to fine powder. H_2O_2 (30%, v/v) and MO were purchased from Fluka Company (Fig. 1). Aqueous solution of

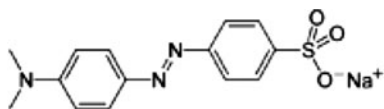


Fig. 1. Chemical structures of MO.

MO was prepared by dissolving a certain amount of MO in deionized water.

2.2. Analysis and procedure

X-ray Diffraction (XRD) pattern of ICW was recorded on Bruker diffractometer equipped with graphite-monochromatized $\text{Cu-K}\alpha$ radiation (Germany). The amount of iron in ICW was determined by acid leaching and analysis of leachate by atomic absorption spectrometer (Varian, Spectra AA 220).

All experiments were conducted in a conical flask (250 mL) placed on an orbital shaker (Stuart scientific, UK) at 200 rpm rotation speed and under dark circumstance. The preselected ICW dose was added to MO aqueous solution and the initial pH was adjusted using H_2SO_4 . Thereafter, H_2O_2 was added to start the experiment. A volume of 5 ml from the solution was taken at preselected time intervals during the reaction and then NaOH was immediately added to the sample. NaOH was added to decompose the residual H_2O_2 and precipitate the formed ferric hydroxide complexes [12]. The precipitated sample was filtered through a $0.45\ \mu\text{m}$ membrane filter before measuring the absorbance at λ_{max} of MO on UV-Visible spectrophotometer (Jasco V530, Japan).

3. Modeling

3.1. Artificial neural network (ANN)

ANN modeling is now used in many areas of engineering, science, and technology. It is considered as a promising tool because of its ability of learning, simulation, and prediction of data [13]. The ANN is an artificial intelligence technique that mimics the human brain's biological neural network in the problem-solving processes [14]. The network consists of numerous individual processing units called neurons, which are connected to a network by a set of weights. The multilayer feed-forward network is a parallel interconnected structure with unidirectional information flow. ANN structure consists of an input layer that includes independent variables, a number of hidden layers, and output layer [15].

In this study, a three-layered back-propagation neural network with tangent sigmoid transfer function (*tansig*) at hidden layer and a linear transfer function (*purelin*) at output layer is used. Neural Network Toolbox V4.0 of MATLAB mathematical software is used for modeling, prediction, and simulation of MO degradation. Out of the several experimental data points generated, 95 experimental data points were used to feed the neural network structure. The experimental

data-set was divided into input matrix $[p]$ and target matrix $[t]$. The input variables were reaction time (t), ICW concentration (mg/L), H_2O_2 dose (mMole), pH, and initial dye concentration. The corresponding MO degradation percent was used as a target. Principal component analysis was performed on input data to filter out the uncorrelated random data.

4. Results and discussion

4.1. XRD characterization of catalyst

The ICW used in this study contains about 90% iron detected. The crystalline structure of iron in the ICW is illustrated in Fig. 2. Iron is crystallized in three phases, magnetite (Fe_3O_4), hematite (Fe_2O_3), and ferrous oxide (FeO).

4.2. Heterogeneous Fenton catalytic activity of ICW

To assess the catalytic activity of ICW as a catalyst in the degradation of MO by heterogeneous Fenton process, preliminary experiments were carried out as follows: (1) presence of H_2O_2 only, (2) presence of ICW, and (3) presence of ICW and H_2O_2 . Degradation of 20 mg/L of MO as function of time is shown in Fig. 3. Low and negligible degradation was achieved in presence of H_2O_2 only and this could be ascribed to limited oxidation ability of H_2O_2 compared with $\cdot OH$ radical. Presence of ICW only achieved MO degradation of 21% in 2 h. This could be ascribed to the adsorption by ICW. It is worth noting that the degradation efficiency of 98% in 2 h was achieved in the presence of catalyst and H_2O_2 , which indicate that ICW reacts with H_2O_2 to generate $\cdot OH$ radicals to degrade MO.

In the present work, two mechanisms were proposed for the generation of $\cdot OH$ radical via

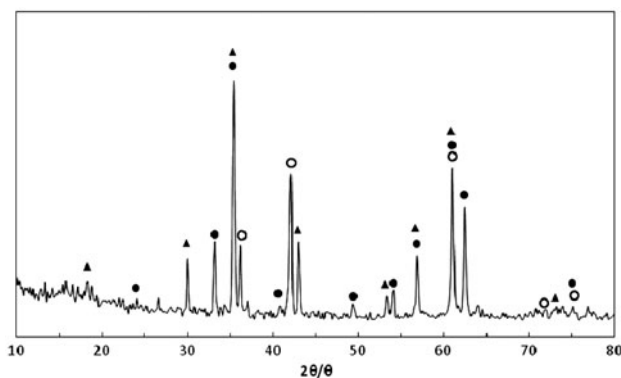


Fig. 2. XRD pattern of Iron in ICW; (▲) magnetite, (●) hematite, and (○) wuestite.

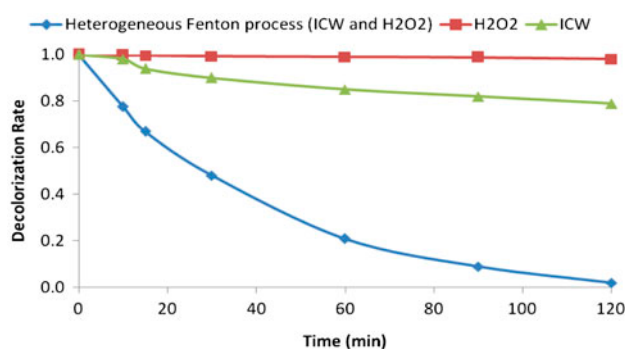
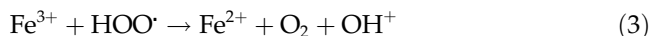
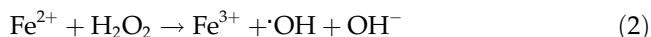


Fig. 3. Degradation rate of MO under different conditions.

Fenton-like reaction using ICW as catalyst. The first mechanism was based on the presence of Fe_3O_4 and Fe_2O_3 oxides which are present in the catalyst as shown in Fig. 2 and is expressed in Eqs. (1)–(3). The other mechanism relied on FeO that is present in the catalyst and is presented in Eqs. (2) and (3). Ferrous ions are continuously generated from the reaction and hence high process performance is expected.



4.3. Effect of pH

The pH of wastewater has an effect on heterogeneous Fenton process performance. The effect of pH on the MO degradation by ICW was investigated at pH range of 2–5. Other operating conditions were 0.15 g/L of ICW dose and 24 of mM H_2O_2 dose. Fig. 4 shows the experimental results which have been compared with the ANN-predicted output. Almost complete degradation of MO was achieved within 60 min at pH 2. However, increasing of pH to 5 resulted in decreased degradation of about 55%. This agrees well with the previously reported results [16]. At pH values above 5, dominant oxidant such as ferryl ion (e.g. FeO^{2+}) may be formed as in Eq. (4) and it is weaker than $\cdot OH$. In addition, deactivation of catalyst with the formation of ferrous/ferric hydroxide complexes leads to the deactivation of ferrous and reduction of $\cdot OH$ [17–19]. In terms of the relation between the experimental results and the predicted values, Fig. 4 shows that the predicted values fairly matched with the experimental data.

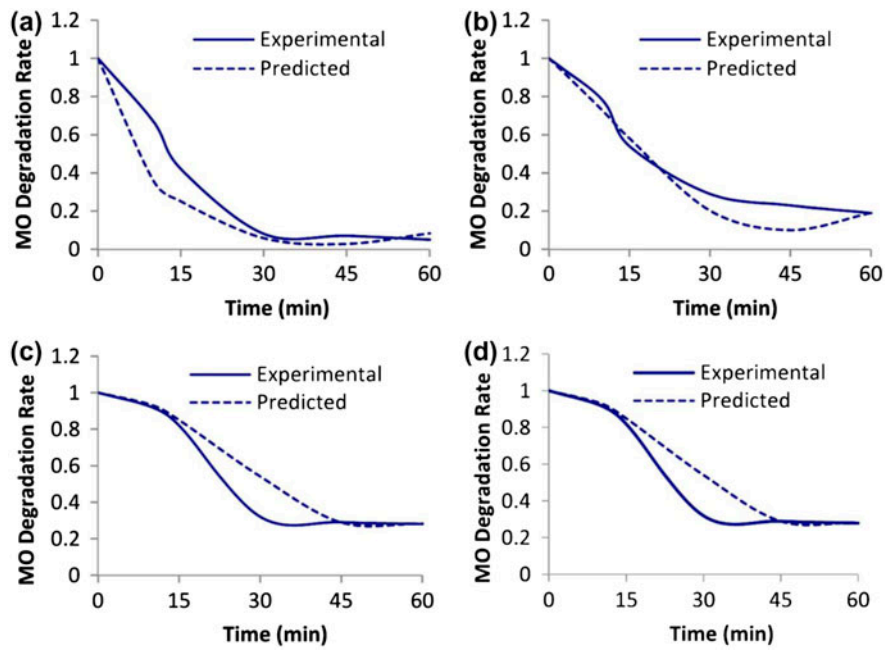


Fig. 4. Effect of pH of solution value on experimental and predicted degradation rate of MO, and pH values (a) 2, (b) 3, (c) 4, and (d) 5.

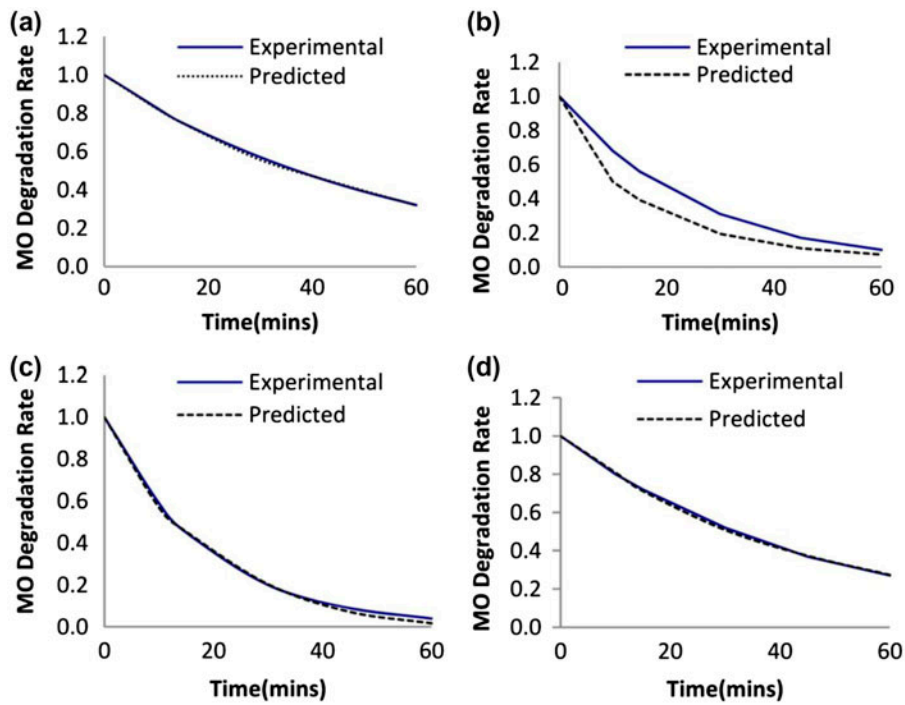


Fig. 5. Effect of hydrogen peroxide concentration on experimental and predicted degradation rate of MO, hydrogen peroxide concentrations (a) 12 mM, (b) 24 mM, (c) 48 mM, and (d) 64 mM.



4.4. Effect of hydrogen peroxide concentration

To study the effects of hydrogen peroxide dose on the MO degradation, H_2O_2 dose was varied in the range of 12–64 mM. Other operating conditions were kept unchanged, 2 for pH and 0.15 g/L of IWC dose. Fig. 5 shows MO degradation as a function of initial H_2O_2 concentration at 20 mg/L of MO. The experimental results have been compared with the ANN-predicted output. As seen in Fig. 5, the rate of MO degradation increases with increasing H_2O_2 concentration during the early stages of reaction; nonetheless, 90% conversion and complete

degradation was achieved after 60 min of reaction for 24 mM of H_2O_2 . An additional run was performed at 48 mM H_2O_2 dose leading to marginal increase in MO degradation. Interestingly, increasing H_2O_2 dose from 24 to 64 mM had an adverse effect on MO degradation which decreased from 90% to about 73%. This could be due to hydrogen peroxide not being selectively converted to $\cdot\text{OH}$ radicals and/or, once $\cdot\text{OH}$ radicals have been generated; they are wasted through scavenging reaction mechanisms. During heterogeneous Fenton reactions, it has been stated that $\cdot\text{OH}$ radicals can partly be scavenged by hydrogen peroxide to form hydroperoxyl radicals (Eq. (5)) with a lower oxidizing power [16]; the latter can also scavenge hydroxyl radicals according to Eq. (6):

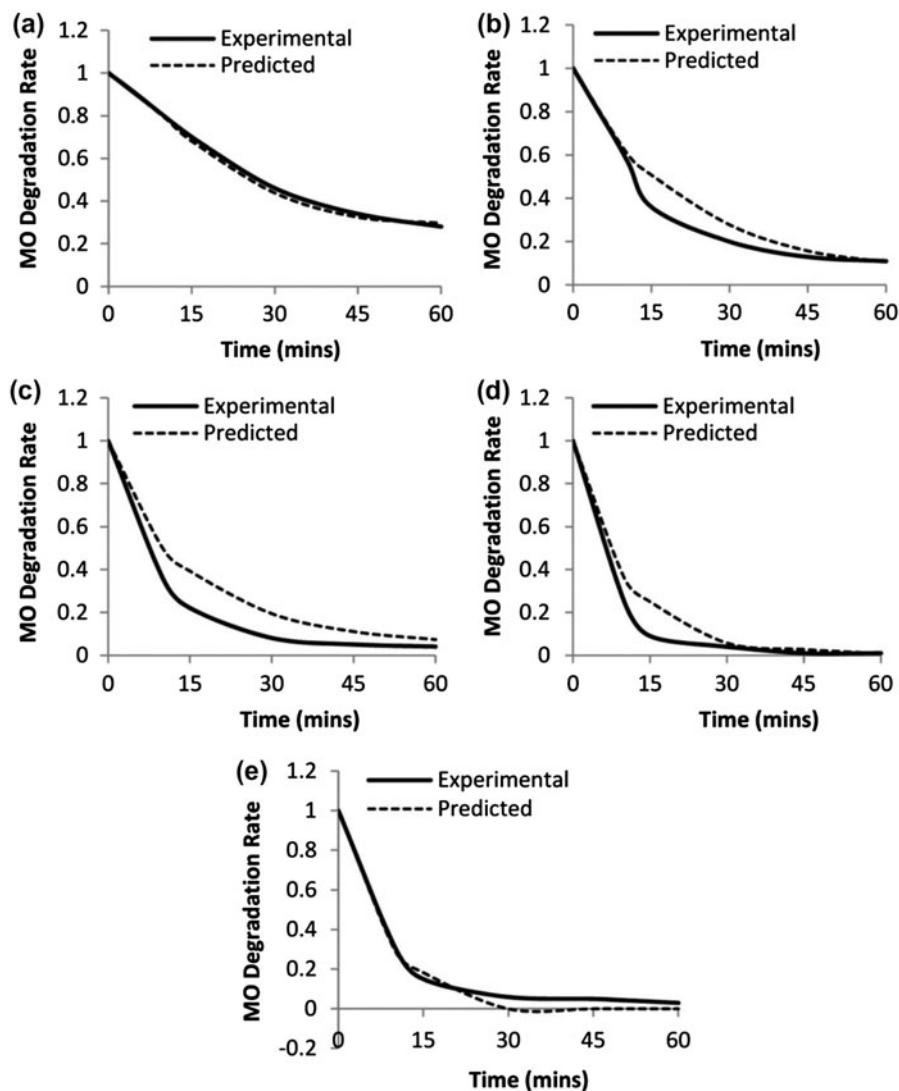


Fig. 6. Effect of ICW concentration on experimental and predicted degradation rate of MO, catalyst doses (a) 0.05 g/L, (b) 0.1 g/L, (c) 0.15 g/L, (d) 0.2 g/L, and (e) 0.25 g/L.

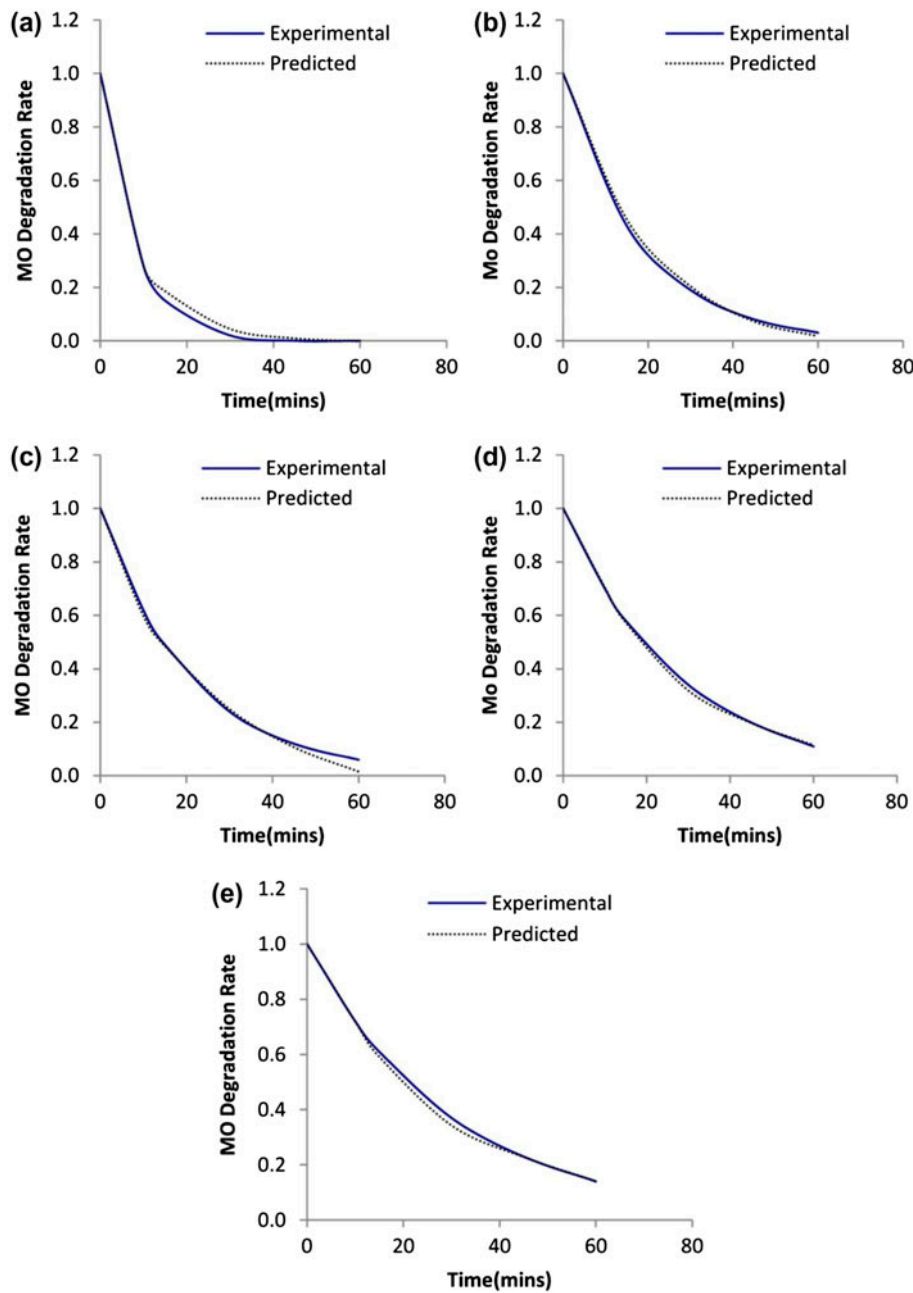
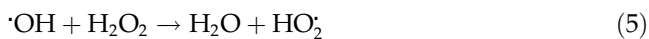


Fig. 7. Effect of MO concentration on experimental and predicted degradation rate of MO, MO concentrations (a) 10, (b) 20, (c) 40, (d) 60, and (e) 80 mg/L.



Hence, 24 mM H₂O₂ dose is considered satisfactory to achieve an acceptable process performance with almost complete MO degradation and it will be considered in the subsequent experiments. In terms of the relation, the experimental results and the predicted

values produced show a good agreement as shown in Fig. 5.

4.5. ICW concentration

The effect of ICW concentration on MO degradation is shown in Fig. 6. The operating conditions were; ICW 0.05–0.25 g/L, MO 20 mg/L, and H₂O₂ dose 24 mM. As seen, the initial MO degradation increased with

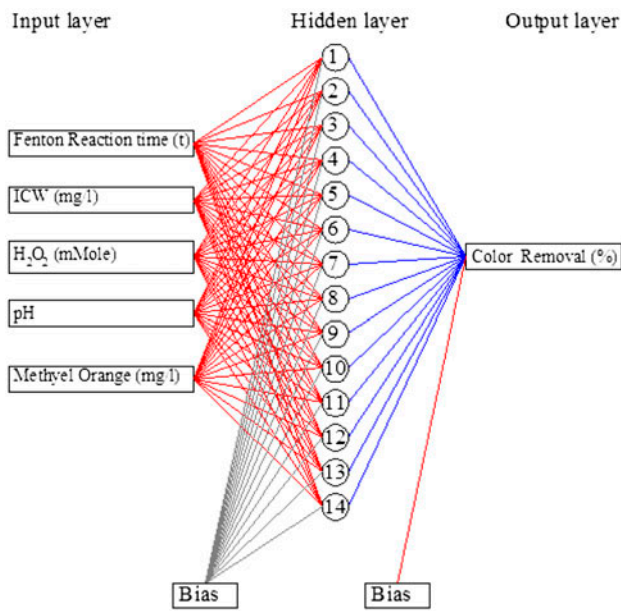


Fig. 8. ANN structure.

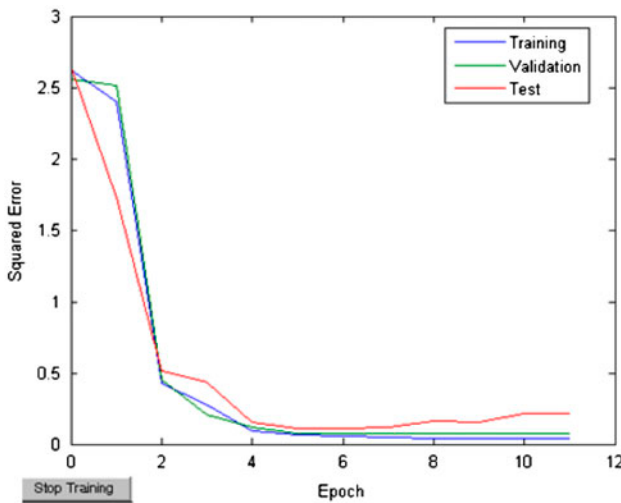


Fig. 9. Relationship between numbers of epoch and MSE for training, validation, and testing of the model.

increasing ICW concentration. Increasing of MO degradation with the increase of ICW concentration was observed, the complete degradation of MO was achieved at ICW concentration of 0.2 g/L after 60 min. Fig. 6 showed that predicted outputs of MO degradation are in good agreement with the experimental values.

4.6. Effect of initial MO concentration

The effect of initial MO concentration in the range 10–80 mg/L on its degradation was studied at 0.2 g/L

ICW concentration and 24 mM H₂O₂ dose, and pH 2. As seen in Fig. 7, degradation decreased with the increasing initial concentration. The final (i.e. after 60 min) MO degradation was 100, 98, 96, 89, and 86% at initial MO concentrations of 10, 20, 40, 60, and 80 mg/L, respectively. Experimental results and predicted values showed good agreement.

4.7. Test and validation of the model

The experimental data-set was divided into training (one half), validation (one fourth), and test (one fourth) subsets, each of which contained 47, 24, and 24 data points, respectively. The experimental data-set was used to feed the ANN to test and validate the model. Topology of an ANN is determined by the number of its layers, number of nodes in each layer and the nature of transfer functions. A three-layered

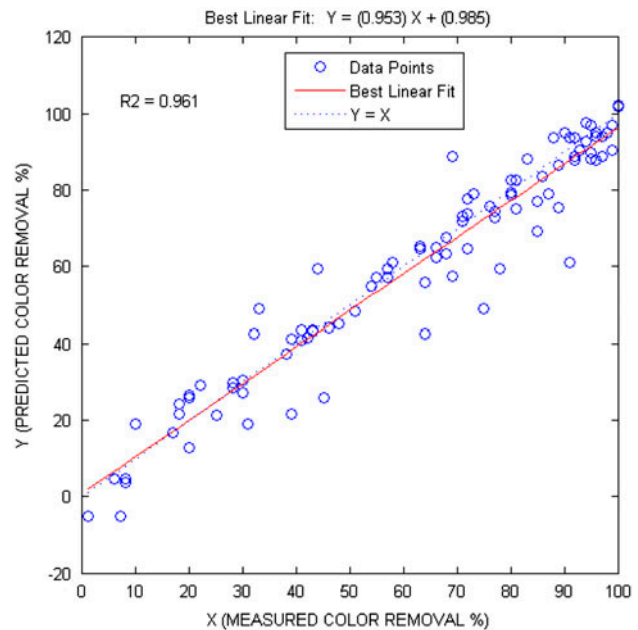


Fig. 10. Comparison between predicted and measured values of the color removal.

Table 1
Relative importance of input variables

| Input variable | Relative importance |
|------------------------------------|---------------------|
| Reaction time | 12.0 |
| ICW concentration | 23.8 |
| H ₂ O ₂ dose | 21.3 |
| pH | 26.8 |
| MO concentration | 16.0 |
| Total | 100.0 |

Table 2
Weights matrix, weight between input and hidden layers (W1), and weight between hidden and output layers (W2)

| Neuron | W1 | | | | | W2 |
|--------|-----------------|-------------------|------------------------------------|---------|------------------|-------------|
| | Input variables | | | | | Output |
| | Reaction time | ICW concentration | H ₂ O ₂ dose | pH | MO concentration | Removal (%) |
| 1 | 0.1082 | −0.2661 | 1.1396 | 0.1492 | 0.2165 | 2.6681 |
| 2 | −0.1132 | −0.3274 | −0.2098 | 2.0264 | −0.5132 | −2.0234 |
| 3 | 0.1893 | −2.8773 | 0.2915 | −0.567 | −0.6523 | −0.4105 |
| 4 | 0.1138 | −0.0002 | 0.3637 | 2.0526 | −1.8296 | −1.7705 |
| 5 | −0.575 | 1.5365 | −0.1729 | −2.073 | 1.1365 | 0.6721 |
| 6 | 0.7323 | 0.2763 | −2.2862 | −1.0635 | −1.061 | 1.1244 |
| 7 | 0.4834 | 0.1921 | −0.555 | 1.3474 | 0.2877 | 1.1827 |
| 8 | −0.0862 | 1.8256 | −0.2339 | −0.0567 | −0.0532 | −2.1011 |
| 9 | 2.0981 | −0.2179 | −0.0788 | 0.765 | −0.5606 | 1.1434 |
| 10 | 1.1553 | −1.9035 | −0.635 | 0.5577 | −0.6075 | 1.1992 |

feed-forward back-propagation neural network with five neurons in the input layer, 10 neurons in the hidden layer and one neuron in the output layer (5-14-1 network) is used for the modeling of MO degradation (Fig. 8). Sigmoid transfer function (*tansig*) between input and hidden layer, and linear transfer function (*purelin*) between hidden and output layer were used. Levenberg–Marquardt back-propagation algorithm was used as a training algorithm for the ANN. Fig. 9 shows the relationship between number of epochs and mean squared error (MSE) for the training, validation, and testing of model. The training stopped when the minimum MSE was 0.039 and number of epochs was 11.

Fig. 10 shows a comparison between the measured and predicted MO degradation percent using the neural network model. The figure contains two lines, one is the perfect fit $Y = X$ (predicted data = experimental data) and the other is the best fit indicated by a solid line with best linear equation $Y = (0.953) X + 0.985$, correlation coefficient (R^2) 0.961, and MSE 0.039.

4.8. Sensitivity analysis

Relative importance of the variables has been assessed using Garson equation [13,20]. The Garson equation is based on the neural net-weight connection weights as in Eq. (7):

$$I_j = \frac{\sum_{m=1}^{N_h} (|W_{jm}^{ih}| \div \sum_{k=1}^{N_i} |W_{km}^{ih}|) \times |W_{mn}^{ho}|}{\sum_{k=1}^{N_i} \left\{ \sum_{m=1}^{N_h} (|W_{km}^{ih}| \div \sum_{k=1}^{N_i} |W_{km}^{ih}|) \times |W_{mn}^{ho}| \right\}} \quad (7)$$

where I_j is the relative importance of the j th input variable on the output variable, N_i and N_h are the numbers of input and hidden neurons, respectively, W s are connection weights, the superscripts “i”, “h”, and “o” refer to input, hidden, and output layers, respectively, and subscripts “k”, “m”, and “n” refer to input, hidden, and output neurons, respectively.

Table 1 shows the relative importance of input variables and Table 2 shows weight matrix, weight between input and hidden layers, and weight between hidden layers and output layers calculated by Garson Eq. (7). All variables (reaction time, Fe concentration, H₂O₂ dose, pH, and MO concentration) have a strong effect on MO degradation. The pH appeared to be the most influential input variables followed by Fe concentration. The low relative importance of MO concentration reveals that the selected operating conditions are valid for a wide range of wastewater strengths [18].

5. Conclusion

- ICW is a feasible catalyst in heterogeneous Fenton process for MO degradation.
- Complete degradation of 20 mg/L of MO was achieved at ICW concentration 0.2 g/L, 24 mM H₂O₂ dose, and pH 2 in 60 min.
- The neural network modeling effectively predicts and simulates the behavior of heterogeneous Fenton process with correlation coefficient (R^2) of 0.961 and MSE of 0.039.
- The sensitivity analysis showed that all studied variables (reaction time, ICW concentration, H₂O₂

dose, pH value, and MO concentration) have strong effect on MO degradation.

- The pH value appeared to be the most influential input variables followed by Fe concentration.

References

- [1] M. Dukkanci, G. Gunduz, S. Yilmaz, R.V. Prihodko, Heterogeneous Fenton-like degradation of Rhodamine 6G in water using CuFeZSM-5 zeolite catalyst prepared by hydrothermal synthesis, *J. Hazard. Mater.* 181 (2010) 343–350.
- [2] P.A. Carneiro, R.F. Pupo Nogueira, M.V.B. Zandoni, Homogeneous photodegradation of C.I. reactive Blue 4 using a photo-Fenton process under artificial and solar irradiation, *Dyes Pigm.* 74 (2007) 127–132.
- [3] Y.M. Li, Y.Q. Lu, X.L. Zhu, Photo-Fenton discoloration of the azo dye X-3B over pillared bentonites containing iron, *J. Hazard. Mater. B* 132 (2006) 196–201.
- [4] E.G. Garrido-Ramirez, B.K.G. Theng, M.L. Mora, Clays and oxide minerals as catalysts and nanocatalysts in Fenton-like reactions—A review, *Appl. Clay Sci.* 47 (2010) 182–192.
- [5] P. Bautista, A.F. Mohedano, J.A. Casas, J.A. Zazo, J.J. Rodriguez, An overview of the application of Fenton oxidation to industrial wastewaters treatment, *J. Chem. Technol. Biotechnol.* 83 (2008) 1323–1338.
- [6] J.Y. Feng, X.J. Hu, P.L. Yue, Discoloration and mineralization of Orange II using different heterogeneous catalysts containing Fe: A comparative study, *Environ. Sci. Technol.* 38 (2004) 5773–5778.
- [7] L.Q. Guo, F. Chen, X.Q. Fan, W.D. Cai, J.L. Zhang, S-doped Fe₂O₃ as a highly active heterogeneous Fenton-like catalyst towards the degradation of Acid Orange 7 and phenol, *Appl. Catal. B: Environ.* 96 (2010) 162–168.
- [8] J.B. Zhang, J. Zhuang, L.Z. Gao, Y. Zhang, N. Hu, J. Feng, D. L. Yang, J.D. Zhu, X.Y. Yan, Decomposing phenol by the hidden talent of ferromagnetic nanoparticles, *Chemosphere* 73 (2008) 1524–1528.
- [9] B. Muthukumari, K. Selvam, I. Muthuvel, M. Swaminathan, Photoassisted hetero-Fenton mineralization of azodyes by Fe(II)–Al₂O₃ catalyst, *Chem. Eng. J.* 153 (2009) 9–15.
- [10] K. Cruz-González, O. Torres-López, A. García-León, J.L. Guzmán-Mar, L.H. Reyes, A. Hernández-Ramírez, J.M. Peralta-Hernández, Determination of optimum operating parameters for Acid Yellow 36 decolorization by electro-Fenton process using BDD cathode, *Chem. Eng. J.* 160 (2010) 199–206.
- [11] H.L. Li, H.Y. Lei, Q. Yu, Z. Li, X. Feng, B.J. Yang, Effect of low frequency ultrasonic irradiation on the sonoelectro-Fenton degradation of cationic red X-GRL, *Chem. Eng. J.* 160 (2010) 417–422.
- [12] L. Xu, J. Wang, A heterogeneous Fenton-like system with nanoparticulate zero-valent iron for removal of 4-chloro-3-methyl phenol, *J. Hazard. Mater.* 186 (2011) 256–264.
- [13] E.S. Elmolla, M. Chaudhuri, M.M. Eltoukhy, The use of artificial neural network (ANN) for modeling of COD removal from antibiotic aqueous solution by Fenton process, *J. Hazard. Mater.* 179 (2010) 127–134.
- [14] E.S. Elmolla, M. Chaudhuri, The use of artificial neural network (ANN) for modelling, simulation and prediction of advanced oxidation process performance in recalcitrant wastewater treatment, in: Chi Leung Patrick Hui (Ed.), *Artificial Neural Networks – Application*, InTech, 2011. Available from: <http://www.intechopen.com/books/artificial-neural-networks-application/the-use-of-artificial-neural-network-ann-for-modelling-simulation-and-prediction-of-advanced-oxidation>
- [15] H. Oguz, A. Tortum, B. Keskinler, Determination of the apparent rate constants of the degradation of humic substances by ozonation and modeling of the removal of humic substances from the aqueous solutions with neural network, *J. Hazard. Mater.* 157 (2008) 455–463.
- [16] H. Hassan, B.H. Hameed, Oxidative decolorization of Acid Red 1 solutions by Fe-zeolite Y type catalyst, *Desalination* 276 (2011) 45–52.
- [17] B.W. Tyre, R.J. Watts, G.C. Miller, Treatment of four biorefractory contaminants in soils using catalyzed hydrogen peroxide, *J. Environ. Qual.* 20 (1991) 832–838.
- [18] S.H. Kong, R.J. Watts, J.H. Choi, Treatment of petroleum-contaminated soils using iron mineral catalyzed hydrogen peroxide, *Chemosphere* 37 (1998) 1473–1482.
- [19] Y. Deng, J.D. Englehardt, Treatment of landfill leachate by the Fenton process, *Water Res.* 40 (2006) 3683–3694.
- [20] G.D. Garson, Interpreting neural-network connection weights, *AI Expert* 6 (1991) 47–51.